A Dissertation on

Theoretical Study of decay processes observed in reactions involving loosely bound projectiles

Submitted towards the partial fulfillment for the

Requirements of the degree of

Masters of Science

in

Physics

Submitted by

Pooja Rani

Roll No.301204005

Under the supervision of

Dr. Manoj K. Sharma

Professor

School of Physics and Materials Science

Thapar University, Patiala-147004

July, 2014

CERTIFICATE

This is to certify that the thesis entitled **"THEORTICAL STUDY OF DECAY PROCESSES OBSERVED IN REACTIONS INVOLVING LOOSELY BOUND PROJECTILES"** being submitted by **Pooja Rani** for the partial fulfillment of the requirements for the award of degree of Masters of Science in Physics at Thapar University, Patiala is a record of the candidate's own work carried out by her under the supervision of **Dr. Manoj K. Sharma, Professor, SPMS** and refers other researcher's work which are duly listed in reference section.

The matter presented in this thesis has not been submitted in part or full for the award of any degree in any university or institute.

Pooja Rani
(Pooja Rani)

Date: 7/7/2014

Dr. Manoj Kumar Sharma

Professor

SPMS, Thapar University

Patiala

Countersigned by:

Dr. Kulvir Singh

(Professor & Head)

SPMS, Thapar University

Patiala

Dr. S.K. Mahopatra

Dean of Academic Affairs

Thapar University

Patiala

I DEDICATE THIS THESIS TO GOD AND

MY FAMILY

ACKNOWLEDGEMENT

I am sincerely thankful and owe my deepest gratitude to M.Sc. thesis supervisor Dr. Manoj K. Sharma, Professor, School of Physics and Materials Science, Thapar University, Patiala. Without him the dissertation would not have been possible. I thank him for his patience and encouragement that carried me on through difficult times and for his insights and suggestions that helped to shape my research skills. His visionary thoughts have influenced me greatly. His dynamical attitude has empowered me with zeal of energy to conquer the minor details of my research work.

I also sincerely thanks to Dr. Kulvir Singh (Professor & Head), School of Physics and Material Science for providing all necessary facilities in the department. I also thankful to all the faculty and staff of the school for their kind support, encouragement and constant moral support to accomplish this task.

I concede my heartiest gratitude to Ms. Gurvinder Kaur, research scholar for the help and valuable suggestions whenever I need it out for her busy schedule.

Special thanks to all my friends at school of physics and material sciences for providing me a friendly environment. I am deeply thankful to my family, their moral support and patient has bared fruit through competition of this thesis.

Patiala

July, 2014

Pooja Rani

Pooja Rani

CONTENTS

List of Figures/Tables

Abstract

The current wave of interest is the reactions where the loosely bound nuclei are involved. These type of reactions involving loosely bound nuclei particularly halo nuclei attracted great interest both from experimentalists and theorists. The reactions with loosely bound nuclei help to find the reaction dynamics and structure of halo nuclei. A reaction does not involve only one process but may evolve variety of decay processes depending on nature of projectile involved and incident energy used in the reactions. For example along with the complete fusion, the contribution of incomplete fusion, direct reaction is also observed in these reactions and an effort is made to address them with the help of dynamical cluster decay model[DCM]. DCM provides information regarding cross sections of all compound nucleus (CN) based decay processes on equal footing and the effect of angular momentum, excitation energy, temperature, deformations and orientations can be duly incorporated wherever applicable. The study of nuclear reactions induced by heavy ions with loosely bound characteristic is also a topic of great interest. The evaporation residue channels are investigated for the low energy heavy ion reactions (^{6}He+^{45}Sc). In ^{6}He+^{45}Sc reaction, the possibility of emission of three fragments (^{5}He, ^{4}He+^{1}n, ER+^{5}He) is analyzed and the behavior of all three fragmentation processes is compared. The behavior of both these is investigated above the Coulomb barrier at highest centre of mass energy. For the reaction (^{6}He+^{45}Sc), the process of complete fusion is taken into account while for the reaction ^{2}H+^{45}Sc three processes- complete fusion, incomplete fusion (^{1}n+^{45}Sc) and direct reaction (P_0=1) is undertaken and their comparative analysis is carried out which imparts useful information regarding the dynamics of loosely bound reactions.

Chapter –I

Introduction

The nucleus is an extremely small, dense object in an atom discovered by Rutherford in the 20th century. Inspite of tremendous amount of information available for atomic nuclei till date, nuclear physics is still a very young science and carries a lot of unexplored aspects. Society favors fundamental research, expecting the benefits that support national as well as human priorities and one of such kind was witnessed in 1896 when Becquerel, while working with photographic plates, accidentally discovered that a mineral (containing uranium) was able to expose the plate while in the dark. Shortly after this, the Curies (Marie and Pierre) isolated two new elements, named polonium and radium, and characterized the radiation they emit. Rutherford and others also found that there are three distinct classes of nuclear radiation, based on their penetrating power called α, β and γ rays. This initial discovery has formed an integral part of nuclear physics and with time proved to be an essential tool for various new advancements. Many medical procedures require radioactive isotopes. Also, nuclear diagnostic techniques have provided us a way to see inside the body without surgery. A prominent application of nuclear research is in developing the long-term means of securing our energy needs within a low-carbon economy thus, showing a great potential for addressing the future needs of nation. The concepts and techniques of nuclear physics have helped to address various other problems such as nuclear power generation, nuclear weapons, nuclear medicine, magnetic resonance imaging, radiocarbon dating etc. These new technologies also found practical applications from integrated circuit production to weapons verification. Tapping into the powerful forces within the nucleus to generate power is a major goal of nuclear scientists and engineers. Revolutionary designs of fission reactors using some novel fuel sources are already being tested. Also, various approaches to nuclear fusion are being developed on an international scale for an ideal environment-friendly solution to our energy needs. Nuclear transmutation is also being investigated as a means of destroying nuclear waste safely. Besides this, acceleration mass spectroscopy is a new technique which can find any nucleus in concentrations below 1 part per trillion. Radioactive dating of the oceans by AMS technique helps in understanding the ocean

circulation patterns. All these High-energy acceleration techniques, reactions and detection methods derived from nuclear physics provide an indispensable set of analytical tools for research, manufacturing and environmental monitoring. Another major motivation for studying the atomic nucleus is simply to gain a fundamental understanding of our world, including its origin, future and the existing state. Nuclear physics can explain much of the evolution of the universe in the first minutes and years after the "big bang".

With these applications and benefits, it is of great interest to study nuclear physics properties and related dynamical aspects. Technological advances, spurred by the demands of nuclear research have inspired us directly to the creation of research and analytical tools. Much of current research relates to the study of nuclei under extreme conditions such as high temperature, excitation energy and angular momentum in low energy region. Recently, the study of loosely bound/ halo nuclei have attained tremendous importance as they form an important aspect in completely understanding the reaction dynamics involved in low energy heavy ion collisions.

Loosely bound nuclei

In mid 1980s, a new feature of the loosely bound nuclei came into picture called Halo nuclei, which lie far from the stability line. The credit of this discovery goes to Tanihata [1-2] for the work of his group at Lawrence Berkeley Laboratory's Bevalac in 1985 on the measurement of the very large interaction cross sections of certain neutron-rich isotopes of helium and lithium and found much larger values for the rms matter radii than would be predicted by normal $A^{1/3}$ dependence. Further in 1987, Johnson and Hansen proposed the large size of these nuclei due to halo effect. The halo is a threshold phenomenon arising from the weak binding of the last one or two valance nucleons and can be described as core surrounded by a veil of dilute nuclear matter, extending into the classically forbidden region. This veil referred to as 'halo' is responsible for much larger radii of these nuclei as compared to normal radius. The strong interaction between protons and neutrons, responsible for the existence of nucleus is short range up to 2fm and vanishes beyond it thus, causing a severe obstacle to experimental investigations related to loosely bound nuclei. Also we know that the average binding energy in a stable nuclei is about 6-8 MeV. But in halo nuclei the binding energy becomes much smaller, in some cases it is less than 1 MeV. Moreover, the life time of halo nuclei is of the order of a millisecond to one second. Thus in reference to halo nuclei, we can say that shell model was unable to explain all the

features that nuclei would show [3].Since halo nuclei are short lived so they must be studied using radioactive beam facilities irradiated on a stable target [4].

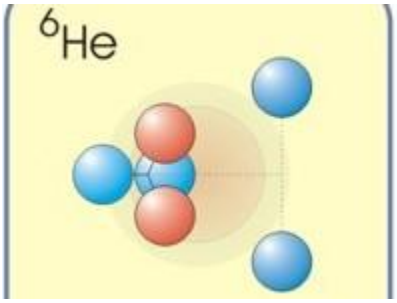

Figure 1.1: The structure of two neutron halo ^{6}He nucleus (the red balls representing protons and blue balls representing neutrons)

Thus the combination of nucleon clustering, low separation energy and the interaction range of strong forces generate the halo nuclei. In addition to decoupling of core and valence particles and their small separation energy, another important criterion for halo nuclei is that the valence particle must be in a low orbit angular momentum state, preferable an *s*-wave, relative to the core since higher *l*-values give rise to a confining centrifugal barrier. The confining Coulomb barrier is the reason why proton halos are not so spatially extended as neutron halos. Much more experimental evidences along with theoretical studies of the nuclei lying at boundaries of the nuclear landscape are required in order to understand the exotic structure, reaction dynamics and various other aspects of reactions involving halo nuclei.

Chart of halo nuclei

The halo nuclei are divided on the basis of neutron rich and proton rich nuclei. The most studied halo nuclei are ^{6}He, ^{11}Li, ^{11}Be. These are the examples of neutron halo system and lie close to the neutron drip line at the limits of particle stability. In recent times, ^{14}Be, ^{14}B, ^{15}C and ^{19}C have also been confirmed as neutron halo nuclei. The nuclei which are still now to be confirmed as halo nuclei are- ^{15}B, ^{17}B, ^{19}B, ^{22}C and ^{23}O. Similarly the existence of proton nuclei include ^{8}B, ^{13}N, ^{17}Ne but these are quite less impressive in terms of extent of their halo part due to their confining Coulomb barrier which holds them closer to the core. Interestingly, the neutron rich nuclei are further classified on the basis of two body bound system and three body bound system. The two body system can be written as core+ valance neutron bounded by short range potential for e.g. ^{11}Be and ^{19}C. Similarly, the three body systems like ^{6}He,^{11}Li can be written as, α+n+n

and are named as Borromean while the light nuclear systems such as ^{5}He, ^{5}Li (α+n, α+p) may be represented as two body system. The clustering in ground state may be unbound since there are no bound states of α+n or n+n (dineutron) systems. By theoretical structure calculations, it was revealed that prominent clustering into fragments such as ^{6,7}Li (α+p+n, α+t) with small inter-cluster separation energy is substantial in light nuclei. The study of reactions involving loosely bound nuclei has been of great interest in recent times. Such reactions may lead to production of equilibrated compound nucleus and its subsequent decay through evaporation residue (ER; A≤4) or fission (symmetric or asymmetric fission) channels. The presence of such nuclei is of great interest and may result into various features such as the suppression or enhancement of the nuclear cross sections for energy region across the Coulomb barrier. Due to extended structure in comparison to ordinary nuclei, relatively easier penetration through the potential barrier is observed, causing enhancement in the cross-sections. On the other hand, such nuclei being loosely bound may also witness an increase in probability of breakup of original projectile and lead to the fusion of residual nucleus (obtained after break-up) with the target nucleus giving rise to suppression in cross-sections and hence the onset of incomplete fusion. These wide variety of phenomenon observed in reactions involving loosely bound nuclei complicate the analysis of experimental data and hence require appropriate theoretical description for proper diagnosis of this exotic phenomenon. The topic of present study is based on the reactions involving loosely bound ^{2}H and ^{6}He nuclei incident on ^{45}Sc target. It is worth mentioning that a deuteron (^{2}H) consisting of a proton and a neutron is the simplest bound state of nucleons, also called simplest halo nucleus while ^{6}He nucleus represented as bound state of α+2n shows a deuteron like cluster structure [5] where the charged core α acts like a proton and the extended halo part (2n) acts like a neutron. The projectile and target involved in the reactions under consideration provide an opportunity to study the complete fusion, incomplete fusion and direct reaction cross-sections in detail. The reactions are given below followed by a brief discussion of the processes in succeeding sections.

$$^{6}_{2}He + \ ^{45}_{21}Sc \rightarrow ^{51}_{23}V \ \rightarrow ^{46}_{21}Sc + \ ^{5}_{2}He \quad \text{(complete fusion)} \ldots (1)$$

$$^{2}_{1}H + \ ^{45}_{21}Sc \rightarrow ^{46}_{21}Sc + \ ^{1}_{1}P \qquad \text{(direct reaction)} \qquad \ldots (2)$$

After break-up of deuteron, deuteron splits up into proton and neutron, then neutron reacts with ^{45}Sc and ICF process takes place.

$$^{1}_{0}n + \ ^{45}_{21}Sc \rightarrow ^{46}_{21}Sc + \ ^{1}_{1}P \qquad \text{(incomplete fusion)} \ldots (3)$$

Heavy ion reactions

The term heavy ion is used for nuclei heavier than the α particle and the reactions involving such projectile beams with incident energy $E_{beam} \leq 15$MeV/ nucleon, are termed as low energy heavy ion reactions (HIR). Various factors such as incident energy, impact parameter, deformations and orientations influence the interaction and hence the dynamics involved in such reactions. At energies above the barrier, heavy ions have smaller wavelength than their radii so a classical picture of heavy ions collisions might be possible. Different types of reactions categorized on the basis of impact parameter are discussed below:-

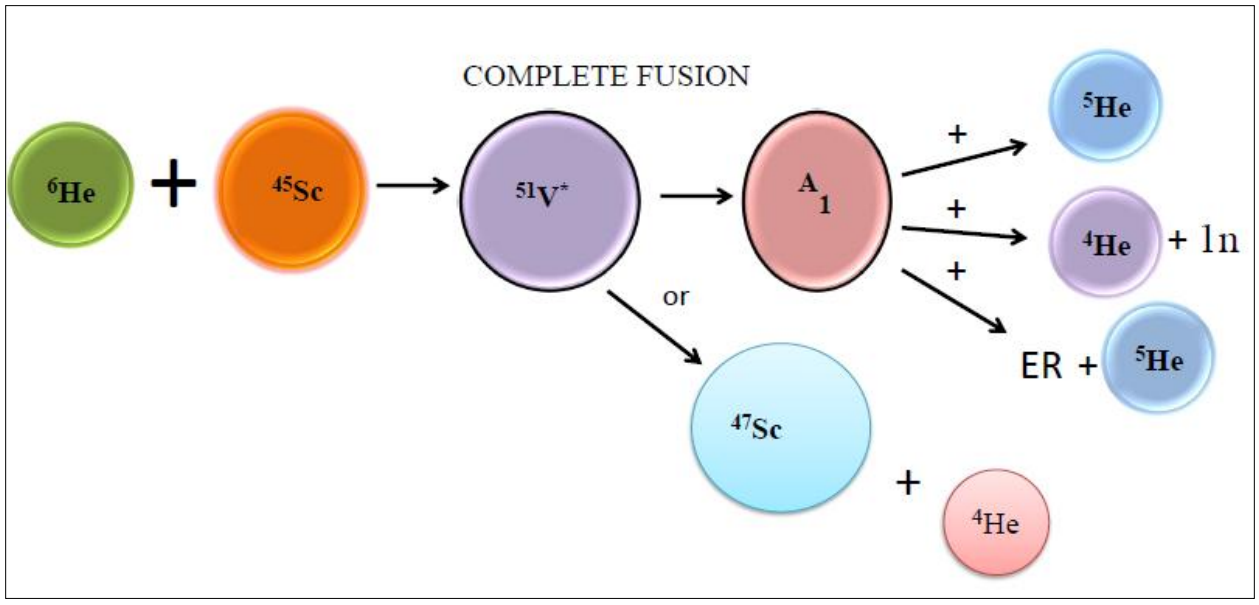

Figure 1.2: A pictorial representation of decay processes observed in ^{6}He induced reaction.

Distant collision

The impact parameter has a significant role in this type of collision. For larger impact parameter, the reaction time is smaller due to which the projectile and the target do not overlap with each other. In these distant collisions, no mass is transferred and the Coulomb forces exclusively determine the elastic scattering and Coulomb excitation processes.

Soft grazing

When the projectile and the target nuclei come in close contact, the nuclear interaction sets in and the process is known as soft grazing. In such collisions, energy and in some cases mass may

also be exchanged but the system retains its original mass asymmetry and kinetic energy. The reactions such as inelastic scattering and direct reactions come under this process.

Hard grazing

When the projectile enters deep into the target nucleus, the collision is called hard grazing. In such collisions, nucleus may be fragmented resulting into massive transfer of a part of a projectile and forming a composite system for a short time leading to incomplete fusion or processes such as deep inelastic collisions. However, for a relatively smaller impact parameter, the projectile may completely fuse with the target nucleus to form a compound nucleus.

The interaction between the nucleons of projectile and target is represented by effective potential which is of three types- the repulsive Coulomb or electrostatic potential, the strongly attractive nuclear potential and the centrifugal potential. The sum of these three terms gives a series of potentials governed mainly through angular momentum ℓ . Thus, the reaction phenomenon may be understood in terms of the angular momentum by converting the impact parameter b into the angular momentum input ℓ using the relation $\ell\hbar=m_p v_p b$. At relatively low energies and corresponding to the values of impact parameters, heavy ion reactions can be classified into complete fusion, incomplete fusion, quassi-fission and deep inelastic collision each of which is explained below and also represented in figure 1.3.

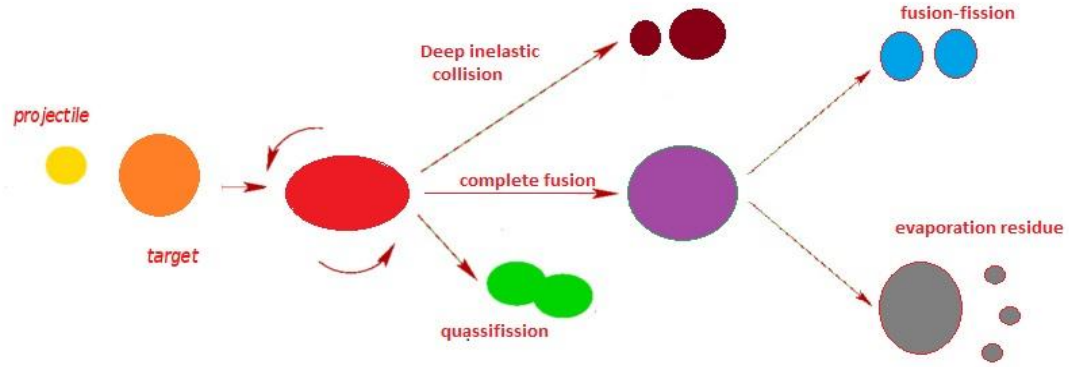

Figure 1.3: Categorization of various decay processes observed in heavy ion reactions.

Complete fusion

There are basically two different ways to form the compound nucleus (CN). One is when the projectile is completely absorbed by the target and the other is when the loosely bound projectile first breaks into the fragments which are successively absorbed by the target nucleus. The first process is called as the direct complete fusion (DCF) and the latter is known as sequential complete fusion (SCF) [6]. Thus, complete fusion may be considered as the sum of direct and sequential fusion of the projectile resulting into the formation of equilibrated compound nucleus (CN). However there also lies the possibility that all the fragments of projectile after break-up do not fuse with the target, resulting into the incomplete fusion (ICF), discussed ahead. When all the nucleons of projectile interact with the target nucleons, the excitation energy is shared statistically among the constituent nucleons due to which the CN remains in excited state for a relatively longer time (10^{-16} sec) compared to relatively shorter period (10^{-22} sec) required by the incident particle to travel past the nucleus. As a consequence, all the memory of entrance channel of compound nucleus is lost and hence the decay process proceeds independent of formation path. The compound nucleus so formed is always in a highly excited unstable state. At this stage, the statistical equilibrium is reached and the average number of excited degrees of freedom becomes constant. Such reactions are called the compound nucleus reactions and are of huge importance in reference to heavy ion collision dynamics. Theoretical and experimental studies of decay products in heavy ion collisions are very significant in establishing the interaction between projectile and target nuclei, subsequent to collision and in studying the role of different reaction mechanisms. Also, they are helpful in providing knowledge about the nuclear processes and structure of the nuclei. The decay of hot and excited CN is considered through emission of evaporation residues [ERs, also called, light particles, $A \leq 4$], complex or intermediate mass fragments [IMFs; $5 \leq A \leq 20$], and fission fragments. Interestingly, ERs are the main reaction products observed for the light mass systems formed in the low energy region heavy ion reactions. For the heavy systems, fission process is responsible for the decay cross sections. However, depending upon the mass of CN formed (A_{CN}), the decay may also consist of one or more of these processes.

Incomplete fusion

Light particle emission from the projectile before interacting with the target may be observed in reactions involving loosely bound projectile, leading to the incomplete fusion process. The projectiles with low break-up threshold split into two fragments, following which only a part of the projectile fuses with the target nucleus while the remaining part moves in the forward direction. The first experimental evidence for ICF was given by Britt and Quinton [7]. This excited composite system formed by the fusion of projectile fragment and target nucleus may also undergo de-excitation by emission of particles or γ rays. Interestingly, the accurate limit to complete fusion and onset of ICF still needs to be defined, but it is observed that the angular momentum, incident beam energy and the distance of closest approach play a crucial role in deciding it. Most of the experiments measure only the total fusion cross section which is the sum of CF and ICF. However for some of the projectile-target combinations, it is also possible to measure cross sections of CF and ICF separately. Some of the examples of such type of reactions are ^{6,7}Li + ^{209}Bi [8-9] and ^{9}Be + ^{208}Pb, [9-10] where the influence of the breakup channel on fusion was shown to be strong. In heavy ion collisions, the study of ICF process has attained a great interest in recent years and the present work also deals with the study of reaction dynamics involved in ^{2}H induced reaction, where ^{2}H (1p,1n) is considered as the simplest case of loosely bound nuclei and breaks up before interacting with the target nuclei. It may be noted that DCM has been successfully applied to reaction involving loosely bound ^{6}Li [11-12] and ^{8}B nuclei, but it is being applied for ^{6}He and ^{2}H induced reaction for the first time.

Quasi-fission

Formation of a composite system, instead of CN may also take place when the projectile hits the target nucleus with energy near the Coulomb barrier. The composite system so formed involves two touching nuclei which interact and exchange nucleons, although their individual identity remains intact [13]. This process is defined as quasi-fission (QF) and is formed in heavy ion collisions in the capture stage of the reaction after dissipation of the kinetic energy [14]. Since quasi-fission involves decay of dinuclear system configuration without formation of compound nucleus, the time scale of emission of fragments is less as compared to CN decay. It is observed mostly in reactions involving symmetric nuclei, leading to heavy or superheavy systems and

hinders the formation of evaporation residue, thus responsible for suppression of ER cross-sections obtained through CN [15]. Experiments on quasifission were recently carried out in Dubna in connection with hot fusion reactions leading to superheavy elements [16-17]. However as an exception, QF has also been observed for some light mass nuclei formed in asymmetric reactions. In the present work, an attempt has been made to address the cross-sections obtained in ^{2}H induced reaction through the direct decay channel.

Direct reactions

Systematic studies of nuclear reactions are essential for comprehensive understanding of nuclear structure, reaction dynamics, underlying nuclear forces and the overall development of nuclear physics. The direct reactions involving excitation of selectively minimal number of nucleonic degrees of freedom also prove to be of great help for such studies. The first quantitative theory of direct nuclear reactions was proposed by S. Butler of Australia in the 1950's and applied to stripping reactions. Majority of nuclear reactions which proceed to a low lying level of the final nucleus receive predominant contributions from a direct process which does not involve the formation of compound nucleus as an intermediate step. As a consequence in the direct reaction dynamics, the structure and properties of the nuclei in the entrance channel have a direct impact on the exit channel contrary to the reactions involving CN formation. Direct reactions are very fast reactions and require projectile energy larger than 5 MeV/nucleon. Also, the projectile and the target nuclei are within the range of nuclear forces for a very short time and the interaction takes place on the surface rather than in the volume of interacting nuclei.

Most direct reactions are of transfer type where one or more nucleons are transferred to or from the incident particle as it passes through the target nucleus. The direct reaction can be studied under two categories (i) direct transfer reactions (ii) direct break-up reactions. The direct transfer reactions are discussed in the following section.

Direct transfer reactions

(a) Pick-up reaction: - in this reaction, the incident projectile strikes with the target and interacts with only few nucleons of the target. The neutron pick-up in the (p, d) reaction forms a suitable example for such reactions.

(b) Stripping reaction: - it is a nuclear reaction in which part of the incident nucleus combines with the target nucleus and the remainder proceeds with its original momentum in original direction without interacting with the target nucleus. For example deuteron stripping (d, p) reactions that have been extensively used to determine nuclear structure and its properties.

The definition of these reactions strongly suggests that the interaction does not occur with the target nucleus as a whole, but with just a part of it. Direct reaction products have highly anisotropic, forward focused angular distributions in the centre of mass reference frame. They are widely used as a tool to study nuclear interactions and nuclear reaction dynamics. These reactions are also important for understanding nucleosynthesis and astrophysics aspects. The detailed investigation of these reactions requires a proper quantum mechanical treatment and the same has been carried out in the present work.

Deuteron induced reactions

A deuteron, having a combination of proton and neutron is a weakly bound system with no excited states, represents a simplest 'halo' nucleus and forms an ideal system for studying the nucleon-nucleon interaction along with nuclear spectroscopic properties. Due to the fact that the center of mass and centre of charge do not coincide, the Coulomb field of target nuclei causes a strong polarization of the deuteron. The weak binding energy of the deuteron (2.224 MeV) is responsible for high complexity of interaction processes that involves a variety of reactions initiated by the neutrons and protons following the deuteron breakup. Therefore the actual calculations and measured data for deuteron-induced reactions are less extensive. Such reactions take place at incident energy of 2-15 MeV and cross section for them are much greater than those of the relevant reactions driven by the charged particles. The distinguishing peculiarity of such reactions is due to deuteron properties. Generally, if the deuteron is absorbed as a whole with high incident energy, the most probable result is the emission of two or more particles, and the simple d-p reaction becomes very unlikely. For E_d>10 MeV, the stripping process still allows an appreciable probability that the proton may carry away all the incident energy leaving behind the neutron in a negative energy (bound) state in the final nucleus. Therefore a neutron bound in the nucleus is called a "negative energy" neutron [18]. The stripping reactions yield relatively fewer negative energy neutrons, but as the deuteron incident energy increases, the neutrons tend to be

more often absorbed with positive energy, causing the immediate re-emission of a neutron. Therefore as the deuteron energy is increased above the Coulomb barrier, the d-p cross section will decline. Thus (d, p) and (d, n) stripping as well as the (d, t) pick-up reaction contributions are important at low incident energies. The deuteron induced direct reaction is shown in figure 1.4 below:-

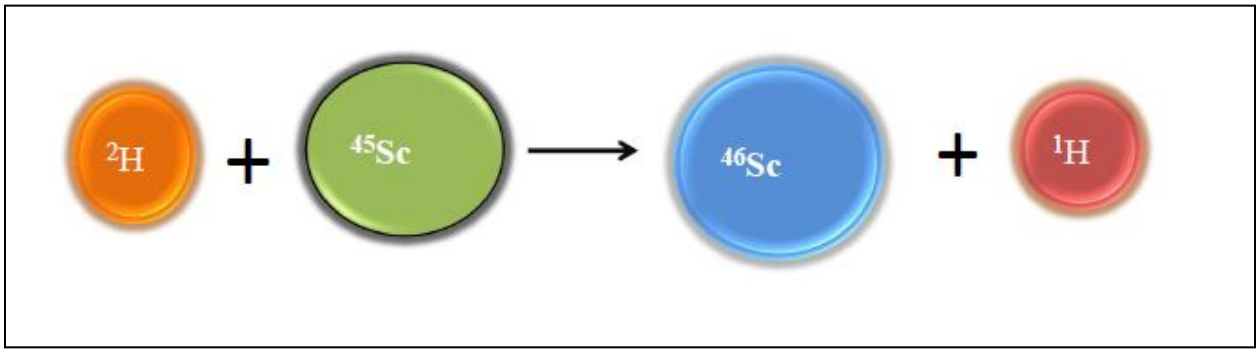

Figure 1.4: Reaction showing interaction of deuteron with ^{45}Sc target.

Oppenheimer process

For reactions involving deuteron as incident projectile, the neutron being uncharged penetrates more easily into the target nucleus rather than deuteron entering as a whole. The sticking probability of the neutron and its penetration probability across the potential barrier is described by the Oppenheimer Phillips process where the proton does not interact with the target nucleus but only carries the surplus energy and momentum with it which is important for an absorption process to occur. Oppenheimer Phillips process is simpler than the ordinary type of nuclear reactions consisting of the formation and disintegration of the compound nucleus [19]. Interestingly, the d-p reactions with o-p scheme are more favorable for heavy nuclei because for the lighter nuclei the potential barrier is so low that it presents no obstacle to the deuteron entering into it nor to the outgoing proton. The example of o-p process is:-

$$^{2}_{1}H + \ ^{45}_{21}Sc \rightarrow ^{46}_{21}Sc + \ ^{1}_{1}P$$

Cross section across the coulomb barrier

For the halo nuclei such as ^{6}He, ^{11}Li, the valance nucleons have low binding energy (0.1-1MeV) and occupy single particle states with low angular momentum (s or p). The wave function of these single particle states of valence nucleons is long and lies outside the potential well. For

reactions involving these nuclei, the structure of halo nuclei affects the reaction mechanisms strongly at energies near the Coulomb barrier. In recent years, a number of experiments have been done to investigate the effect of projectile structure in reactions induced by the halo nuclei on the reaction mechanisms, at energies around and below the Coulomb barrier. Also, the effect of halo structure on the fusion reaction is worth studying because the presence of such nuclei affects the shape of the projectile-target potential, thus reducing the Coulomb barrier as a result of which an increment in the fusion cross section is observed. It is due to long range of the radial wave functions of the valence nucleons that static effects are observed. On the other hand, dynamical effects are observed due to the coupling of the relative motion of the projectile and target nuclei. A lot of theoretical studies are made for understanding these dynamical effects on the fusion cross section with halo nuclei. Corresponding to the different ideologies, different models are predicted to explain the effect of halo nuclei on reaction mechanisms. For example to explain fusion cross sections, according to continuum-discretised coupled-channel (CDCC) calculations, there is increment in total fusion (complete+incomplete) cross-section with respect to the no coupling case. Also from the experimental point of view, different groups did not reach the same conclusion about the enhancement or suppression effect on the fusion cross section due to the projectile halo structure. The mechanisms of reactions in the above barrier region may be different from the below barrier region [20]. In the present work, we used the dynamical cluster decay model (DCM) based on the quantum mechanical fragmentation theory to study the impact of loosely bound projectiles ^{6}He and ^{2}H on ^{45}Sc target so as to have the idea about governance of such light mass nuclear reactions and associated dynamical aspects which may impart useful information about general behavior of such nuclei.

References

[1] I. Tanihata et al., Phys. Rev. Lett. **55** (1985) 2676.

[2] I. Tanihata et al., Phys. Lett. B **160** (1985) 380.

[3] J. Al-Khalili , Lect. Notes Phys. **651** (2004) 77–112.

[4] Thesis by Riccardo RAABE on study of low energy reactions with the Halo nucleus ^{6}He, Katholieke Universiteit Leuven (2001).

[5] N. K. Skobelev, A. A. Kulko, V. Kroha, V. Burjan, Z. Hons, A. V. Daniel et.al., J. Phys. G: Nucl. Part. Phys. **38** (2011) 035106.

[6] H. D. Marta, L. F. Canto, and R. Donangelo, Phys. Rev. C **89** (2014) 034625.

[7] H. C. Britt and A. R. Quinton, Phys. Rev. **124** (1961) 877.

[8] M. Das Gupta, D. J. Hinde, K. Hagino, S. B. Moraes, P. R. S. Gomes, R. M. Anjos, R.D. Butt, A. C. Berriman, N. Carlin, C. R. Morton *et al.*, Phys. Rev. C **66** (2002) 041602 (R)

[9] M. Das Gupta, P. R. S. Gomes, D. J. Hinde, S. B. Moraes, R. M.Anjos, A.C.Berriman, R. D. Butt, N. Carlin, J. Lubian, C. R.Morton *et al.*, Phys. Rev. C **70** (2004) 024606.

[10] M. Das Gupta, D. J. Hinde, R. D. Butt, R. M. Anjos, A. C.Berriman, N. Carlin, P. R. S. Gomes, C. R. Morton, J. O. Newton, A. Szanto de Toledo *et al.*, Phys. Rev. Lett. **82** (1999) 1395.

[11] Gudveen Sawhney, Manoj K Sharma and Raj K Gupta, J. Phys. G: Nucl. Part. Phys. **41** (2014) 055101

[12] Gurvinder Kaur and Manoj K. Sharma, Physical Review C **87** (2013) 044601.

[13] V. V. Volkov, Phys. Rep. **44** (1978) 93.

[14] S. A. Kalandarov, G. Adamian, N. V. Antonenko, A. Diaz Torres and W. Scheid, Nuclear Theory'22 (ed. V. Nikolaev), Heron Press, Sofia, (2003).

[15] T. K. Ghosh, Proceedings of the DAE Symp. On Nucl. Phys. **56** (2011) 33.

[16] M. G. Itkis et al. Report (JINR, Dubna) **E 15** (1999) 99-248; Proc. *7*th Int. Conf. on Clustering Aspects of Nuclear Structure and Dynamics (eds. M. Korolija, Z. Basrak, R. Caplar;World Scientific, Singapore) p. **386** (2000).

[17]. Proc. Int. Symposium on Exotic Nuclei (eds. Yu. E. Penionzhkevich and E. A. Cherepanov; World Scientific, Singapore) p. **143** (2001); Int. Conf. on Nuclear Physics at Border Lines (eds. G. Fazio *et al.*; World Scientific, Singapore) p. **146** (2002);

[18] D. C. Peaslee, Phys. Rev. **74** (1948) 9.

[19] H. A. Bethe, Phys. Rev. **53** (1938) 39.

[20] M Fisichella, V Scuderi, A Di Pietro, P Figuera, M Lattuada et.al., Journal of Physics: Conference Series **282** (2011) 012014.

Chapter-II

Methodology

Great interests have been shown by the theorists and experimentalists for several decades to understand the formation and decay of a compound nucleus. This provides us information regarding cross section of fusion, ER, fusion-fission process and helps to understand the dynamics involved in a reaction. On the basis of compound nucleus formed in low energy heavy ion reaction, Evaporation residue is the dominating decay process for $A \leq 80$ and for heavy mass systems ($A \geq 200$), fission is dominating process where the contribution of ER is small. In the present work, we have studied two reactions as follows:-

$$^{6}He + {}^{45}Sc \rightarrow {}^{51}V^{*} \rightarrow A_1 + A_2 \quad \text{(complete fusion)} \qquad \ldots..(1)$$

$$^{2}H + {}^{45}Sc \rightarrow {}^{46}Sc + p \quad \text{(direct reaction)} \qquad \ldots. (2)$$

In the first reaction, the calculations of the production cross sections for ^{46}Sc and ^{47}Sc are performed by experimentalists using EMPIRE code 2.18. Similarly in the second reaction, the calculations of the production cross sections for ^{46}Sc are performed using the EMPIRE 2.18 and TALYS 1.2. According to EMPIRE 2.18, the reaction proceeds through the formation of a compound nucleus while TALYS 1.2 gives satisfactory agreement only close to the Coulomb barrier. Thus in order to have clear picture of decay mechanism involved, attempts has been made to analyze the reactions theoretically using dynamical cluster decay model [1-6] which is the extended form of the preformed cluster model (PCM)[7-8]

Since, deformation and orientation degree of freedom play an important role in the decay of nuclear system so it is necessary to investigate the role of deformations and its effect on the formation and decay process of compound nucleus. Further, when the compound nucleus is formed, the temperature, excitation energy and angular momentum effects also come into picture. All these features have been duly incorporated in the DCM and used to study the decay of hot ($T \neq 0$) and rotating ($\ell \neq 0$) composite system. This method is based on the quantum mechanical fragmentation theory (QMFT) [9-12] which provides us information about nuclear structure and reaction dynamics. Interestingly, DCM treats all the decay processes equivalently

(evaporation residues ($Z_2 \leq 2$, $A_2 \leq 4$), intermediate mass fragments ($5 \leq A_2 \leq 20$) and fission fragments) on equal footing as collective mass motion of preformed cluster or fragments through the interaction barrier. The DCM supports this explanation only in terms of the modified shape of potential inside the barrier which is an in built feature of the DCM and can be explained by fitting the neck-length parameter (ΔR). Two types of configurations are investigated in DCM-hot 'equatorial' and cold 'polar' configurations [13].

DCM can be applied successfully to decay of light mass, heavy mass and superheavy compound systems over a wide range of energies. It can be worked out in terms of collective coordinates of the mass (and charge) asymmetries $\eta = (A_1 - A_2)/ (A_1 + A_2)$ (and $\eta_Z = (Z_1 - Z_2)/ (Z_1 + Z_2)$), the relative separation R, the multipole deformations $\beta_{\lambda i}$ (λ = 2, 3, 4...) and orientations $\theta_{i,}$(i=1,2) of two nuclei or fragments. Using these coordinates, in terms of partial waves, the compound nucleus decay or the fragment production cross section is given as:-

$$\sigma = \frac{\pi}{k^2}\sum_{\ell=0}^{\ell max}(2\ell + 1)P_0P \qquad \ldots\ldots (3)$$

Where value of k is given by: - $k=\sqrt{\frac{2\mu E_{c.m}}{\hbar^2}}$ and reduced mass

$$\mu = \left[\frac{A_1A_2}{(A_1+A_2)}\right]m = \frac{1}{4}Am(1 - \eta^2) \qquad \ldots\ldots (4)$$

Apparently, for ℓ=0 (s-wave), $\sigma = \frac{\pi}{k^2} P_0P$ which is an equivalent of decay constant of $\lambda = \nu_0P_0P$. In other words, we can say that σ_0 and λ differ only through a constant. P_0 is preformation probability and it tells about the missing nuclear structure and enters DCM as a solution of stationary Schrodinger equation. The advantage of P_0 is that it not only gives the total fusion cross section but also tells about the individual contribution of its components (ER, IMF, FF, and QF) and depends on η motion. The penetrability P refers to R motion. Both η and R refers to the nucleon division and exchange between the outgoing fragments. So the kinetic energy of the incoming channel is transferred to internal excitation of the outgoing channel where the internal excitation can be written as:-

$$E^*_{CN} = E_{c.m.} + Q_{in} \qquad \ldots\ldots\ldots (5)$$

The excitation energy E_{CN} is related to temperature T as:-

$$E_{CN}^{*} = \left(\frac{A}{9}\right)T^{2} - T \qquad \text{…….... (6)}$$

For the ICF process a part of the projectile interacts with the target nucleus. Thus P_0 is calculated in the same way as the CN process except that the composite system formed in ICF (due to the break-up of original projectile) is different. In the present work, the reaction under consideration is:-

$$^{2}H + {}^{45}Sc \rightarrow {}^{46}Sc + p$$

After break-up of deuteron, the deuteron breaks up into proton and neutron. Neutron reacts with ^{45}Sc and for the ICF process the reaction changes to

$$^{1}n + {}^{45}Sc \rightarrow {}^{46}Sc + p$$

Here, the energy of projectile need to be changed in reference to new projectile and can be obtained by applying appropriate energy correction.

$$E_{Projectile} = \frac{E}{A} * A^{T} \qquad \text{…….... (7)}$$

Where A is the mass of compound nucleus and A^T is the mass of projectile before breakup.

The energy of the fragment which does not strike with the target and moves straight in direction can be calculated as:-

$$E_{fragment} = \frac{E}{A} * A^{F} \qquad \text{…….... (8)}$$

Here A^F is mass of the fragment which goes straight without striking.

Using the above equation (7) and (8), the energy of the projectile after break up can be written as:-

$$E_{ICF}^{P} = \frac{E}{A} * A^{T} - \frac{E}{A} * A^{F} \qquad \text{…….... (9)}$$

It must be noted that ICF process comes into picture for higher angular momentum values say $\ell \geq \ell$crit. and absence of potential pocket forbids fusion until a part of the projectile is released to provide input angular mometa [14].

For the direct reaction, the entrance channel is considered to keep its identity and the preformation probability is taken unity (P_0=1) for the decaying fragment.

P_0 is the solution of stationary Schrodinger equation η, at a fixed R=R_a,

$$\left\{-\frac{\hbar^2}{2\sqrt{B_{\eta\eta}}}\frac{\partial}{\partial\eta}\frac{1}{\sqrt{B_{\eta\eta}}}\frac{\partial}{\partial\eta}+V_R(\eta,T)\right\}\psi^{\nu}(\eta)=E^{\nu}\psi^{\nu}(\eta) \quad \text{…….....} (10)$$

With ν = 0, 1, 2, 3 . . . referring to ground-(ν=0) and excited state solutions, with the ground state P_0 given as:-

$$P_0=\sqrt{B_{\eta\eta}}\mid \psi[\eta(A_i)]\mid^2 (\tfrac{2}{A}) \qquad \text{…….....} (11)$$

The mass parameters $B_{\eta\eta}$ are the smooth hydrodynamical masses [15] and represent the kinetic energy part in eqn (10). The P in equation (3) refers to penetration probability and is calculated using the WKB integral as:-

$$P=\exp[-\frac{2}{\hbar}\int_{R_a}^{R_b}\{2\mu[V(R)-Q_{eff}]\}^{1/2}dR] \qquad \text{…....} (12)$$

Here, R_a is the first turning point of the penetration path for the decay of hot CN used for calculating the penetrability P, and is given as

$$R_a = R_1(\alpha_1, T) + R_2(\alpha_2, T) + \Delta R(\eta, T) \qquad \text{…….....} (13)$$

$$= R_t(\alpha, T) + \Delta R(\eta, T)$$

And the radius vector can be defined as:-

$$R_i(\alpha_i,T)=R_{0i}(T)[1+\sum_{\lambda}\beta_{\lambda i}Y_{\lambda}^{0}(\alpha_i)] \qquad \text{…….....} (14)$$

The nuclear radii R_{0i} of the spherical nuclei (dependent on temperature) can be defined as [16]:-

$$R_{0i}= [1.28A_i^{1/3}-0.76+0.8A_i^{-1/3}] (1+0.0007T^2) \quad \text{……..... (15)}$$

R_b is the second turning point and used to solve equation (12) and can be written as:-

$$V (R_a) =V (R_b) = Q_{eff} =TKE (T). \quad \text{……..... (16)}$$

The scattering potential can be represented as:-

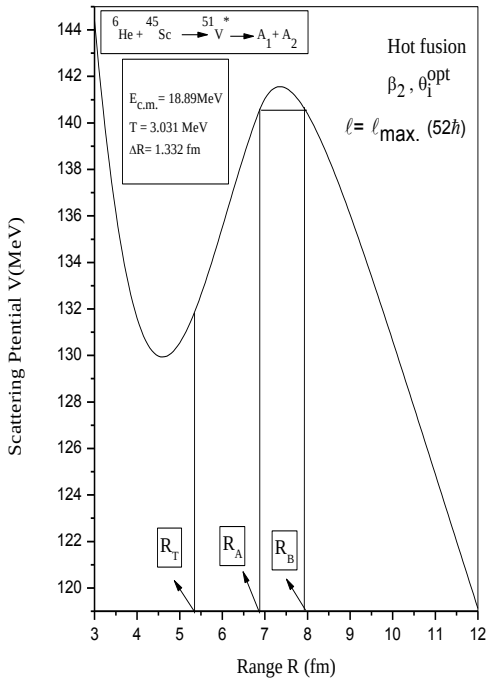

Fig. 2.1. Variation of scattering potential as a function of range R plotted for the decay of $^{51}V^*$ nucleus formed in ^{6}He induced reaction.

The fragmentation potential $V_R(\eta, T)$ that goes in Schrodinger equation can be defined as:-

$$V_R(\eta,T) = \sum_{i=1}^{2}\left[V_{LDM}(A_i,Z_i,T)\right] + \sum_{i=1}^{2}\left[\delta U_i\right]\exp(-T^2/T_0^2) + V_c(R,Z_i,\beta_{\lambda i},\theta_i,T) \quad \text{……..(17)}$$
$$+V_P(R,A_i,\beta_{\lambda i},\theta_i,T) + V_\ell(R,A_i,\beta_{\lambda i},\theta_i,T)$$

Where V_C, V_P, and V_ℓ are, respectively, the temperature and orientation dependent Coulomb, nuclear proximity, and angular momentum dependent potentials.

The proximity potential defined when two surfaces approach each other is expressed as:-

$$V_P(A_i, \beta_{\lambda i}, \theta_i, T) = 4\pi \bar{R}(T)\gamma b(T)\Phi(S_0(T)) \quad \text{.....(18)}$$

Where $\bar{R}(T)$ and $\phi(s_o, T)$ represents the inverse of the root mean square radius of Gaussian curvature and universal function respectively.

Similarly, Coulomb potential defines the force of repulsion between two nuclei and for deformed nuclei it can be written as:-

$$V_C = \frac{Z_1 Z_2 e^2}{R} + 3Z_1 Z_2 e^2 \sum_{\lambda,i=1.2} \frac{1}{2\lambda+1} \frac{R_i^{\lambda}(\alpha_i)}{R^{\lambda+1}} Y_{\lambda}^{(0)}(\theta_i) \left[\beta_{\lambda i} + \frac{4}{7}\beta_{\lambda_i}^2 Y_{\lambda}^{(0)}(\theta_i)\right] \quad \text{... (19)}$$

Here Z is the atomic numbers of projectile and target and $\beta_{\lambda i}$ (λ=2, 3, 4…) defines deformations. The T-dependent liquid drop energy V_{LDM} (T) is that of [17], with (seeger's) constants at T=0 refitted to give binding energies of [18], defined as B= V_{LDM} (T=0) + δU. The shell corrections are calculated in the empirical method of Myers and Swiatecki [19].

References

[1]] B. B. Singh, M. K. Sharma, R. K. Gupta, W. Greiner, Int. J. Mod. Phys.E1 **5** (2006) 699; B. B. Singh, M. K. Sharma, R. K. Gupta, Phys. Rev. C **77** (2008) 054613.

[2] M. K. Sharma, G. Sawhney, S. Kanwar, R. K. Gupta, Mod. Phys. Lett. A **25** (2010) 2022; M. K. Sharma, G. Sawhney, J. Phys. G: Nucl. Part. Phys. **38** (2011) 105101.

[3] R. Kumar, K. Sandhu, M. K. Sharma, R. K. Gupta, Phys. Rev. C **87** (2013) 054610; K. Sandhu, M. K. Sharma, R. K. Gupta, Phys. Rev. C **85** (2012) 024604; K. Sandhu, M. K. Sharma, R. K. Gupta, Phys. Rev. C **86** (2012) 064611.

[4] M. Kaur, M. K. Sharma, and R. K. Gupta Phys. Rev. C **86** (2012) 064610 ; M. Kaur and M. K. Sharma ibid. **85**, 054605 (2012); M. Kaur, R. Kumar, M. K. Sharma, ibid. **85** (2012) 014609.

[5] G. Kaur and M. K. Sharma, Nucl. Phys. A **884** (2012) 36 ; G. Sawhney, M. K. Sharma, Eur. Phys. J. A **48** (2012) 57.

[6] G. Kaur and M. K. Sharma, Phys. Rev. C **87** (2013) 044601; G. Kaur, D. Jain, R. Kumar, M. K. Sharma, Nucl. Phys. A **916** (2013) 260; G. Sawhney, G. Kaur, M. K.Sharma and R. K. Gupta, Phys. Rev. C **88** (2013) 034603.

[7] D.N. Poenaru and W. Greiner, J. Phys. G: Nucl. Part. Phys. **17** (1991) S443.

[8] S. S. Malik and R. K. Gupta, Phys. Rev. C **39** (1989) 1992.

[9]R.K.Gupta,W.Greiner,in:W.Greiner,R.K.Gupta(Eds.),HeavyElementsandRelatedNewPhenomenon,vol.I,WorldScientific,Singapore,1999,p.**536**,Chapter14.

[10] J. Maruhn, W. Greiner, Z. Phys. **251** (1972) 431; R. K. Gupta, W. Scheid, W.Greiner, Phys. Rev. Lett. **35** (1975) 353.

[11] R. K. Gupta, M. K. Sharma, S. Singh, R. Nouicer, C. Beck, Phys. Rev. C **56** (1997) 3242; R. K. Gupta, M. K. Sharma, N. V. Antonenko, W. Scheid, J. Phys. G, Nucl. Part. Phys.**25** (1999) L47; M. K. Sharma, R. K. Gupta, W. Scheid, J. Phys. G, Nucl. Part. Phys. **26** (2000) L45.

[12] J. Maruhn and W. Greiner, Phys. Rev. Lett. **32** (1974) 548.

[13] Manoj K Sharma and Gurvinder Kaur, Pramana-J.phys.,**82** (2014) 5.

[14] A Yadav, V. R. Sharma, Pushpendra P. Singh et. al., Phys. Rev. C **86** (2012) 014603.

[15] H. Kroger, W. Scheid, J. Phys. G: Nucl. Part. Phys. **6** (1980) L85.

[16] G. Royer and J. Mignen, J. Phys. G: Nucl. Part. Phys. **18** (1992) 1781.

[17] N. J. Davidson, S. S. Hsiao, J. Markram, H. G. Miller and Y. Tsang, Nucl. Phys. A **570** (1994) 61C

[18] G. Audi and A. H. Wapstra, Nucl. Phys. A **595** (1995) 4.

[19] W. Myers and W. J. Swiatecki, Nucl. Phys. A **81** (1966) 1.

Chapter-III

Results and Discussions

In the past few years, a lot of experimental work has been devoted to study reactions induced by loosely bound nuclei and halo nuclei in order to investigate the effect of incident projectile on nuclear structure and reaction mechanism [1]. Experiments carried out using exotic nuclei are helpful in studying CF reaction cross sections at different projectile energies below and above the Coulomb barrier. Also, the incomplete fusion (ICF) process observed due to the low break-up threshold and its influence on fusion cross-section has been studied using the halo nuclei by various scientific groups around the globe. In general the extended structure of the halo nuclei results in the increase of fusion cross section whereas on the other hand if we take into account the breakup channel of loosely bound nuclei resulting in ICF process then fusion cross section get equivalently reduced. In general, the description of breakup reactions at low beam energies is more difficult because one cannot ignore the finite excitation energies. Some authors have adopted a coupled channel approach, which is the conventional method used to describe low energy, heavy ion reactions of ordinary nuclei. For halo nuclei, this requires a discretization of continuum states [2-4]. A lot of experimental work has been done in reactions induced by ^{6,7}Li [5].In view of these anomalous features, in present work, we intend to investigate the influence of halo nuclei on the contribution of fusion and other competing reaction processes using dynamical cluster decay model. The reactions under consideration involving halo projectiles are:

$$^{6}He + {}^{45}Sc \rightarrow {}^{51}V^{*} \rightarrow A_1 + A_2 \quad \text{(complete fusion)} \qquad \ldots..(1)$$

$$^{2}H + {}^{45}Sc \rightarrow {}^{46}Sc + p \qquad \text{(direct reaction)} \qquad \ldots. (2)$$

After break-up of deuteron, it splits into proton and neutron and then the neutron reacts with ^{45}Sc.

$$^{1}n + {}^{45}Sc \rightarrow {}^{46}Sc + p \qquad \text{(incomplete fusion)} \qquad \ldots..(2)$$

The internal structure of deuteron and the lightest halo nucleus ^{6}He [6] has attracted much interest in recent times. It must be noted that the behaviour of ^{6}He can also be studied through direct nuclear reactions [7] but here, we analyze its behaviour through compound nuclear

reactions. So in order to study these various reaction mechanisms and cross-sections as per the experimental data, the calculations have been done using the dynamical cluster decay model (DCM) [8-12] which is based on the well known quantum mechanical fragmentation theory [QMFT]. Since the deformation and orientation degree of freedom are explicitly included in DCM, the cross-sections have been calculated by taking quadrupole (β_2) deformations within optimum orientation approach into account.

Initially, the work presented here is focused on the results obtained through the decay of $^{51}V^*$ system formed in reaction induced by ^{6}He nucleus. In reference to the experimental data of [13], the decay of compound nucleus $^{51}V^*$ has been studied using DCM by calculating the cross-sections for the emission of ^{5}He fragment and α-particle at three different energies lying above the Coulomb barrier. To study the structure of $^{51}V^*$ system, the variation of fragmentation potential and preformation probability has been plotted as a function of fragment mass A_2 for both the decay fragments i.e. ^{5}He and ^{4}He, the former discussed first.

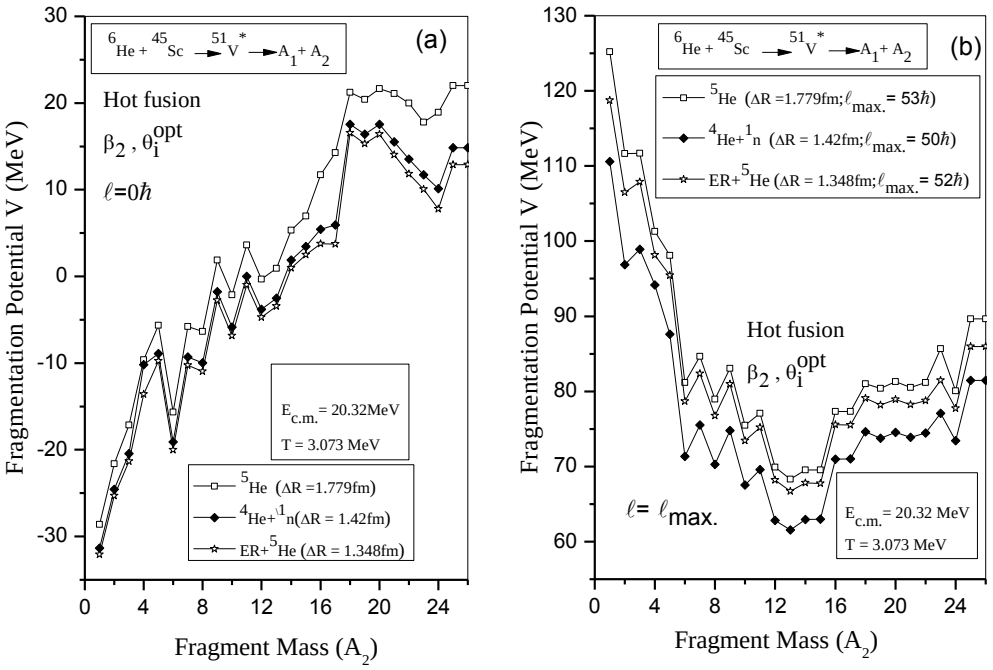

Fig.3.1 The variation of fragmentation potential as a function of fragment mass (A_2) for the decay of $^{51}V^*$ nucleus formed in ^{6}He induced reaction using β_2 deformed fragmentation at $E_{c.m.}$=20.32 MeV plotted for (a) ℓ =0ħ (b) $\ell = \ell_{max.}$

To obtain the measured cross-sections for ^{5}He decay channel, calculations have been done within single parameter fitting of DCM, the neck-length parameter ΔR for the use of quadrupole (β_2) deformed fragmentation approach. This means that at a given incident energy, the reported cross sections have been calculated for the best value of ΔR. For the ^{5}He decay cross-sections it has been observed that even for the maximum allowed value of ΔR, the experimentally measured cross-sections have not been achieved. The value of ΔR, the corresponding maximum angular momentum ℓ_{max}, decided at a point where the ERs cross-section tends to be negligible, ER→ 0, and the maximum cross-sections obtained for it have been tabulated in Table1. It is clearly evident from this that in addition to ^{5}He, other fragments or combination of different fragments may also contribute towards the decay of ^{51}V* nucleus. Thus the cross-section for A=5 and Z=2 have been studied by considering A=1+4 and Z=0+2 instead of ^{5}He alone. Interestingly, within this approach, the DCM calculations could approach the measured cross-sections at relatively much smaller ΔR values which are also tabulated in Table1. However, no significant difference is observed in ℓ_{max} values for all three energies.

Further, since in light mass nuclei, as the one under consideration, the ER decay mode is more dominant. So an attempt has also been made to observe the contribution of ERs (fragments with mass upto A=4) in addition to the measured ^{5}He fragment. The relevant details are also tabulated in Table1 and comparative analysis of all the three choice of decay channels are discussed ahead through variation of fragmentation probability and preformation probability. It may be noted that since the behavior of fragmentation potential and preformation probability observed for decay channels was similar at all considered energies, the graphs have been shown at higher, above barrier energy, $E_{c.m.}$ = 20.32 MeV (T=3.073 MeV) only.

In Fig 3.1, the variation of fragmentation potential as a function of fragment mass A_2, is shown at $E_{c.m.}$=20.32MeV for extreme values of angular momentum i.e. $\ell = 0\hbar$ and $\ell = \ell_{max}$. This figure representing the relative behavior of all three decay channels helps to understand the emission of most favorable decay fragments for the decay of $^{51}V^{*}$ system. It is observed that at $\ell = 0\hbar$ (see fig. 3.1(a)), with increase in fragment mass (A_2), the fragmentation potential increases however at higher ℓ -value i.e $\ell = \ell_{max}$ (see fig. 3.1(b)), the fragmentation potential decreases till a certain mass (A_2 =13) and increase thereafter. The structure of potential energy surfaces (PES) change under the effect of angular momentum

suggesting that ER process is dominant at lower angular momentum states whereas emission of heavier fragments starts operating with increase in ℓ values. It is observed that at ℓ = 0, the magnitude of fragmentation potential is maximum for ^{5}He, followed by ^{4}He+1n and ER+^{5}He decay channel. This result seems to suggest that ER+^{5}He or ^{4}He+1n are more probable decay channels as compared to ^{5}He decay paths. A closer look however suggests that ER+^{5}He is most dominant among the three. A similar trend in magnitude of fragmentation potential is also

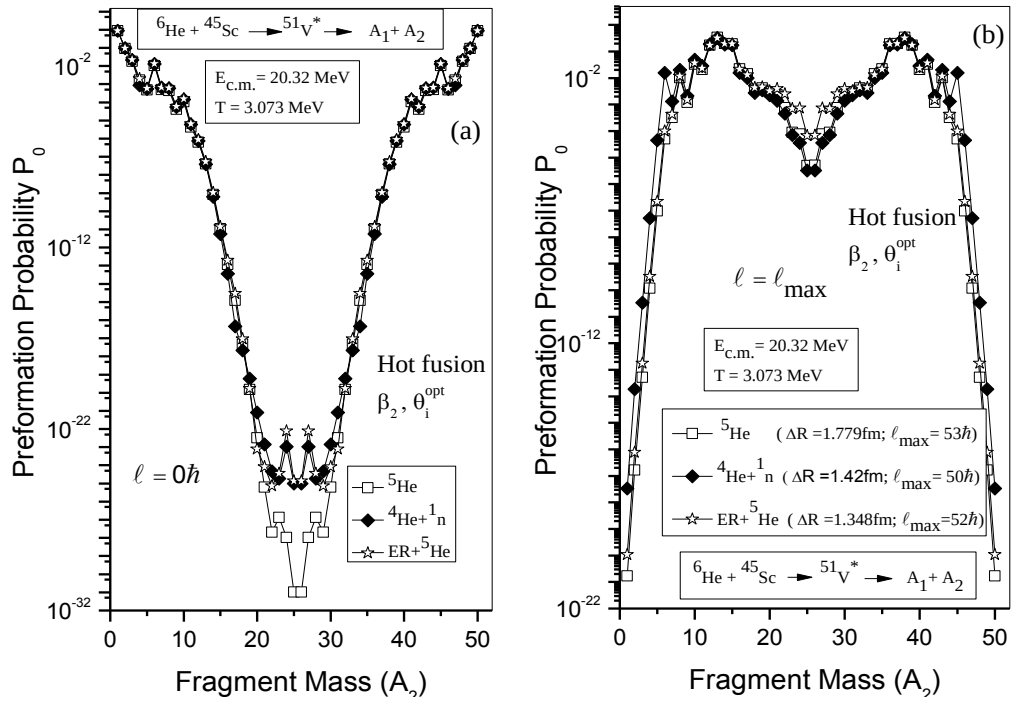

Fig 3.2 The variation of preformation probability (P_0) plotted as a function of fragment mass (A_i; i=1,2) at maximum energy $E_{c.m.}$ = 20.32 MeV for (a) ℓ =0ħ (b) ℓ = ℓ_{max}

observed at higher ℓ i.e. ℓ =ℓ_{max}.with an exception that ^{4}He +1n seems most preferred channel here. But as ER process is dominant only at lower angular momentum states, one may conclude that ER+^{5}He is perhaps the most preferred channel in the decay process. It must be noted that, in DCM calculations the minimum fragmentation potential corresponds to the maximum preformation probability which indicates more favorable decay as compared to the ones with higher fragmentation potential. The contribution of ER cross-sections, constituting of 1n, 2n, 3n

and ^{4}H fragments almost saturates the measured experimental cross-sections at all three energies while for the other competing ^{4}He+1n decay channel, 1n contributes most in attaining the measured cross-sections.

After observing the variation of fragmentation potential, the preformation probability (P_0) is plotted as a function of fragment mass (A_i; i=1, 2) in Fig, 3.2. From the figure it is observed that mass distribution remains asymmetric at extreme values of angular momentum for all the three decay channels. Also unlike the fragmentation potential, no considerable difference is observed in the magnitude of preformation probability, despite of significant difference in the associated neck-length values. As mentioned earlier, for light mass nuclei the behavior at lower ℓ -values is more important, hence at minimum ℓ, the preformation probability of light particles is maximum and that of intermediate mass fragments and fission fragments is minimum while the trend is reverse for higher ℓ. At a much deeper insight, it is observed that, at $\ell=0\hbar$ for the fission region, the preformation probability for all three decay channels start deviating particularly for ^{5}He

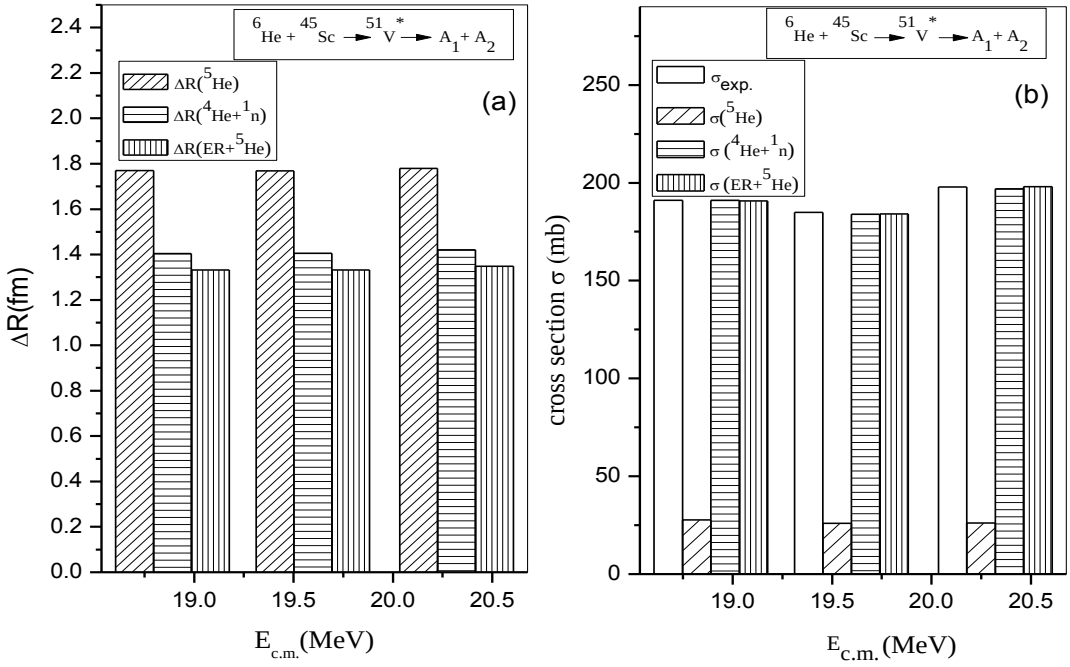

Fig 3.3 (a) The best fit neck length parameter (ΔR) for the decay of light mass nucleus $^{51}V^{*}$, plotted as a function of center-of-mass energy $E_{c.m.}$ (b) The corresponding cross-sections

obtained using DCM for all three decay channels shown as a function of $E_{c.m.}$, in comparison to the experimental data.

channel but it does not carry much significance as magnitude is negligibly small. DCM is a non-statistical description and is based on a single parameter fitting, the neck-length parameter, ΔR. Fig.3.3 (a) shows the best fit values of ΔR plotted for the decay of light mass $^{51}V^{*}$ nucleus for three different decay approaches, i..e ^{5}He, ^{4}He+1n and ER+^{5}He. It is observed that the value of ΔR is maximum for the ^{5}He decay, relatively smaller for ^{4}He+1n channel and least for the most favorable ER+^{5}He channel. The trend of variation of ΔR associated with different decay channels is independent of incident energy of projectile. Moreover, neck-length value is almost independent of centre of mass energy. Further, Fig.3.3 (b) shows the cross-sections calculated using DCM for the use of ΔR values plotted in Fig.3.3 (a). The cross-section for the ^{5}He decay channel, with maximum ΔR is least while it is in agreement with the experimental data for both ^{4}He+1n and ER+^{5}He decay channel. This observation further supports the fact that the measured cross-section favour the decay in form of ER+^{5}He and ^{4}He+1n channels.

Table 1- The decay cross sections for different channels calculated using DCM for the $^{51}V^{*}$ nucleus formed in the ^{6}He + ^{45}Sc reaction with the inclusion of quadrupole deformation at three different center-of-mass ($E_{c.m}$) energies, compared with experimental data. Also, the $\ell = \ell_{max}$ values are tabulated.

Energy $E_{c.m.}$(MeV)	Decaying fragment	ΔR(fm)	$\ell_{max.}$	$\sigma_{DCM(mb)}$	$\sigma_{exp.(mb)}$
18.891	^{5}He	1.770	53$\hbar$	27.7	191± 21
18.891	^{4}He+^{1}n	1.404	50$\hbar$	191	191± 21
18.891	ER+^{5}He	1.332	52$\hbar$	190.70	191± 21
19.597	^{5}He	1.769	53$\hbar$	26.01	184± 20
19.597	^{4}He+^{1}n	1.405	50$\hbar$	184	184± 20
19.597	ER+^{5}He	1.332	52$\hbar$	184.04	184± 20
20.32	^{5}He	1.779	53$\hbar$	26.1	197± 20
20.32	^{4}He+^{1}n	1.42	50$\hbar$	197	197± 20
20.32	ER+^{5}He	1.348	52$\hbar$	198	197± 20

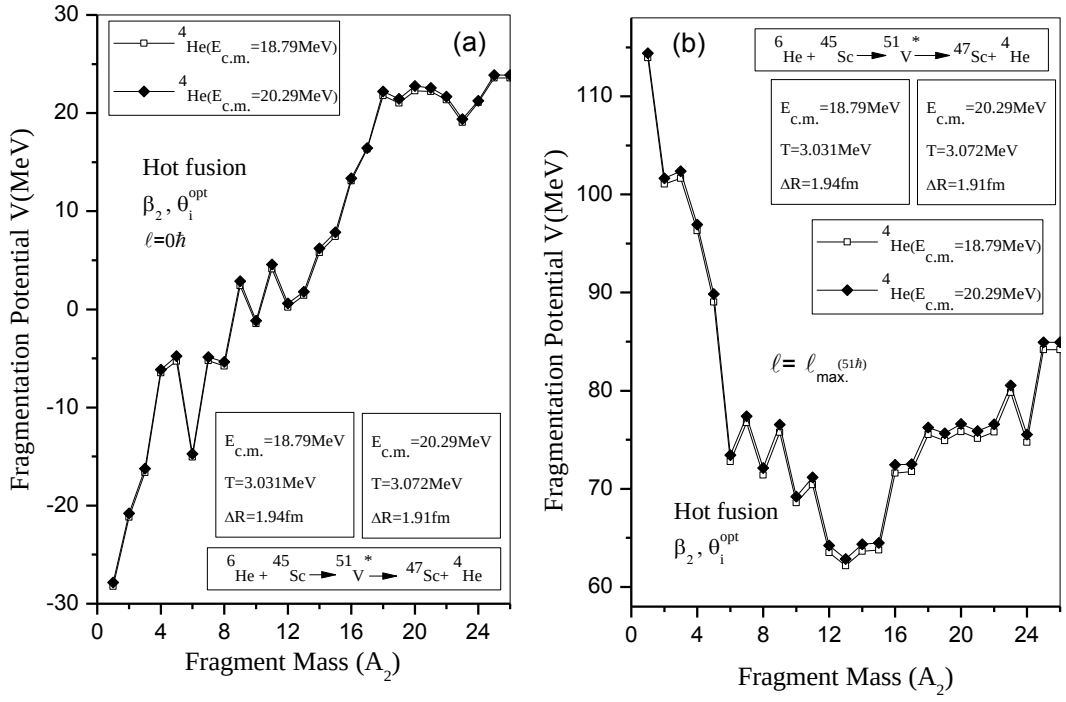

Fig 3.4 Fragmentation potential as a function of fragment mass (A_2) for the decay of $^{51}V^{*}$ nucleus through emission of α-particle with the inclusion of β_2 deformed fragmentation at $E_{c.m.}$=18.79 MeV and $E_{c.m.}$=20.29 MeV at (a) ℓ =0$\hbar$ (b) ℓ = $\ell_{max.}$

Apart from the decay channels studied above, the experimental cross-sections are also available for emission of another fragment, ^{4}He from the excited $^{51}V^{*}$ nucleus formed in ^{6}He induced reaction. In the present work, the dynamical cluster decay model has also been applied to calculate the decay cross-sections of ^{4}He at different energies in order to have better understanding of the reaction mechanism involving halo nuclei. Fig 3.4 shows the variation of fragmentation potential as a function of fragment mass A_2 at two energies ($E_{c.m.}$ =18.79 MeV and Ec.m. =20.29 MeV) both lying above the Coulomb barrier. Interestingly, no effect of energy is observed at extreme ℓ-values on the PES. Thus, one may conclude that, structure of fragmentation potential observed for the emission of α-particle is independent of the choice of energy. From the figure it is evident that with increase in fragment mass A_2, increase in the fragmentation potential is observed for ℓ =0$\hbar$ while decrease in magnitude of potential is observed at higher ℓ, i.e ℓ_{max}. This observation is in agreement with the fragmentation projectile

of A=5 fragment depicted in fig. 3.1. It must be noted that the α-cluster structure is visible for both ℓ-values. The cross-sections are found to approach the measured data within the error limits.

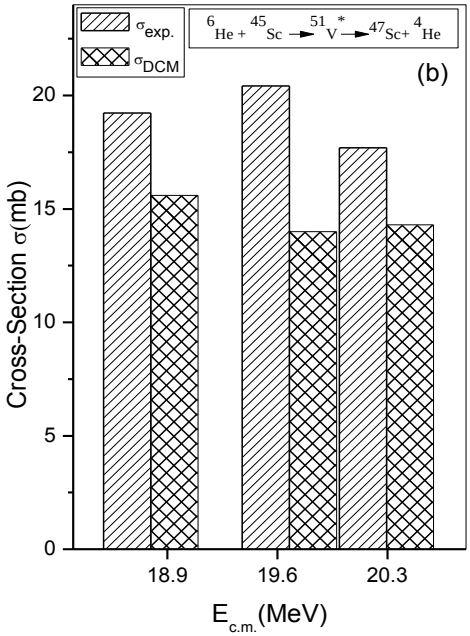

Fig 3.5 (a) ^{4}He cross-sections plotted as a function of $E_{c.m.,}$ for the reaction ^{6}He + ^{45}Sc → $^{51}V^{*}$→ ^{47}Sc + ^{4}He by taking into account β_2 quadrupole deformations compared with experimental data.

Table 2- The α-decay cross sections of for the reaction ^{6}He + ^{45}Sc → $^{51}V^{*}$ reaction calculated by using β_2 deformed fragmentation approach at three $E_{c.m.}$ values, compared with the experimental data. The ΔR and ℓ_{max} values used are also given in the table.

Energy $E_{c.m.}$(MeV)	ΔR(fm)	$\ell_{max.}$	$\sigma_{DCM(mb)}$	$\sigma_{DCM(mb)}$
18.794	1.94	51$\hbar$	15.6	19.230 ± 4.2
19.676	1.90	51$\hbar$	14.0	20.427± 5.8
20.294	1.91	51$\hbar$	14.3	17.699± 4.5

The neck-length parameter used to calculate the α–decay cross-sections are shown in table 2. One may see that, ΔR remains almost constant independent of the energy involved. Using the

best fit values of ΔR, the cross-sections obtained are found to have nice agreement with the experimental data (with error limits) and are shown in fig. 3.5 and also after studying various CN decay channels for reaction induced by halo nuclei, ^{6}He, we have also analyzed the dynamics involved and the effect on decay mechanisms for reaction involving simplest halo nucleus ^{2}H, as projectile on ^{45}Sc target,

$$^{2}H + {}^{45}Sc \rightarrow {}^{46}Sc + p \qquad \text{(direct reaction)}$$

This direct reaction behaves as a simplest case of stripping reaction, involving interaction of n-constituent of loosely bound deuteron, with the target nucleus. To account for this behavior of loosely bound nucleus, the preformation probability for the fragments to be emitted i.e. ^{46}Sc + p is considered unity and is referred as direct reaction (DR). Another approach implied in DCM to calculate the cross-sections is by considering break-up of loosely bound ^{2}H into n and p. Due to this break-up, incomplete fusion (ICF) is observed, where only n interacts with the target nucleus while p goes un-interacted as spectator. To calculate the cross-section for this ICF process appropriate energy correction is involved to obtain energy of n, being used as projectile. In addition to this, there also lies some possibility of ^{2}H + ^{45}Sc leading to compound nucleus (CN), which may subsequently decay by emitting p. Thus, a comparative analysis of all the three processes is carried out. The neck-length parameter used and the cross-sections obtained through them are tabulated in Table 3. The calculations have been done by taking quadrupole deformed fragmentation within optimum orientation approach. The calculated results find reasonable agreement with available data [13]. The comparative analysis of decay processes is carried out at three energies covering whole range of measured data.

Table 3- DCM calculated relative contribution of various decay processes for the emission of p observed in the ^{2}H induced reaction (^{2}H + ^{45}Sc → ^{46}Sc + p) , obtained by taking quadrupole deformation at different $E_{c.m.}$. The energy for ICF process obtained after energy correction is also tabulated. In addition to this the comparison with measured experimental data is shown along with the ΔR and ℓ_{max} values involved. It must be noted in the table that the cross sections of proton at lowest energy are found to be enhanced as compared to experimental data for direct reactions.

Reaction type	$E_{c.m.}$(MeV)	T(MeV)	ΔR(fm)	$\ell_{max.}$	$\sigma_{DCM(mb)}$	$\sigma_{DCM(mb)}$
CN	0.745	1.952	0.16	28 $\hbar$	0.00138	0.00134 ±0.00030
DR	0.745	1.952	0.0	28$\hbar$	4.42	0.00134± 0.00030
ICF	0.380	1.438	0.321	25$\hbar$	0.00133	0.00134 ±0.00030
CN	5.543	2.185	1.340	31$\hbar$	367	366± 80
DR	5.543	2.185	0.689	31$\hbar$	366	366± 80
ICF	2.832	1.606	1.24	31$\hbar$	365	366 ±80
CN	11.10	2.425	1.363	31$\hbar$	208	208± 43
DR	11.10	2.425	0.731	31$\hbar$	208	208 ±43
ICF	5.672	1.780	1.276	31$\hbar$	208	208 ±43

Fig.3.6 shows the variation of fragmentation potential as a function of A_2 for all the three above mentioned decay processes at highest energy $E_{c.m.}$=11.10MeV, T=2.425MeV for CN and direct reaction whereas, $E_{c.m.}$=5.672MeV, T=1.780MeV obtained after energy correction for the incomplete fusion process. The calculations have been done with the inclusion of β_2 deformation. Independent of ℓ values, the PES for all the three process is almost similar and show asymmetric mass distribution. The α-cluster structure seems in operation for all the processes. The magnitude of fragmentation potential is found to be minimum for the direct reaction process and maximum for CN mechanism. This observation seems to suggest that the decay of ^{2}H induced reaction is more favorable through direct reaction mechanism and the possibility of formation of CN channel is rather small.

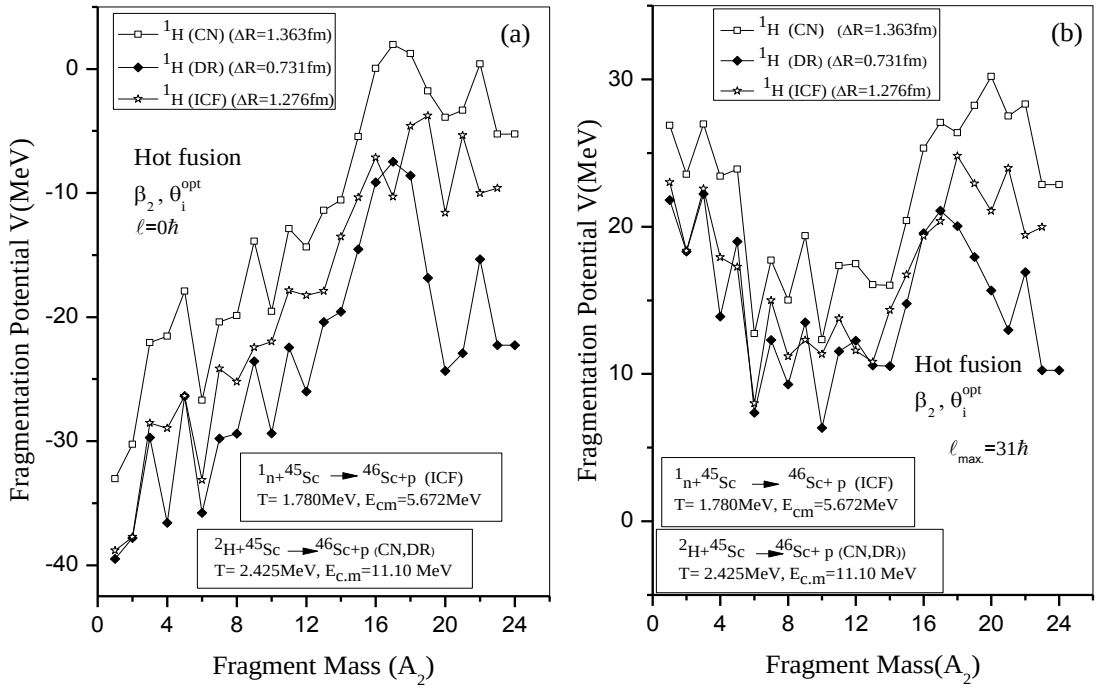

Fig 3.6 Comparison of fragmentation potential as a function of A_2 for the three processes (complete fusion, incomplete fusion, direct reaction) shown at highest energy at (a) ℓ =0ħ (b) $\ell = \ell_{max.}$

In summary, the DCM has been successfully applied to study the reaction mechanisms involved in loosely bound reactions. For the reactions involving ^{6}He and ^{2}H projectiles incident on ^{45}Sc target, the decay of CN and the composite system, other than CN have been studied. The cross-sections for the decay of $^{51}V^*$ nucleus have been studied by taking quadrupole deformation within optimum orientations into account for three different decay channels, ^{5}He, ^{4}He+1n and ER+^{5}He. It has been observed that in addition to the experimental, measured ^{5}He the ER fragments are also favorable for the decay of light mass $^{51}V^*$ nucleus. Further the DCM calculated cross-sections for α-particle have also been attained in nice agreement with the experimental data, with in the error limits. It has been observed that the structure of fragmentation projectile is independent of choice of incident energy. In addition to this, the decay of composite system formed in ^{2}H induced reaction has been studied by taking three different decay channels. It has been considered that d incident on ^{45}Sc target undergoes stripping process, and hence the preformation probability of decay fragments ^{46}Sc+p being emitted is considered unity. Moreover, the decay through incomplete fusion and complete fusion

is also observed. It has been observed that decay through direct reactions is more favorable for this reaction. It will be of further interest to investigate such reactions induced via loosely bound projectiles to have comprehensive idea about nuclear dynamics involved and structural features governed in the light mass region.

References

[1] Alessia Di Pietro, Journal of Physics: Conference Series **205** (2010) 012042.

[2] Y. Sakuragi, M. Yahiro, and M. Kamimura, Prog. Theor. Phys. Suppl. **89** (1986) 136 ; Y. Hirabayashi and Y. Sukaragi, Phys. Rev. Lett. **69** (1992) 1892

[3] C. A. Bertulani and L. F. Canto, Nucl. Phys. **A539** (1992) 309c.

[4] C. H. Dasso, S. M. Lenzi, and A. Vitturi, Nucl. Phys. **A639** (1998) 635; Phys. Rev. C **59** (1999) 539 .

[5] J. Cruz, H. Luis, M. Fonseca, Z. Fulop et.al., J. Phys. G: Nucl. Part. Phys. **35** (2008) 014004 (6pp)

[6] Tanihata I et al. , Phys. Rev. Lett. **55 (**1985) 2676.

[7] Y. L.Ye, D.Y.Pang, G.L. Zhang, D X Jiang, T. Zheng et.al., J. Phys. G: Nucl. Part. Phys. **31** (2005) S1647–S1653

[8] S. Kanwar, M. K. Sharma, B. B. Singh, R. K. Gupta, W. Greiner, Int. J. Mod. Phys E **18** (2009) 1453.

[9] R. K. Gupta, Clusters in nuclei, C. Beck (Ed.), Lecture notes in Physics, vol. **818**,vol. I, springer- Verlag, Berlin, Heidelberg, (2010), p.223;

S. K. Arun, R. Kumar, R. K. Gupta, J. Phys. G, Nucl. Part. Phys. **36** (2009) 085105.

[10] D. Jain, R. Kumar, M. K. sharma, R. K. Gupta, Phys. Rev. C **85** (2012) 024615.

[11] M. K. Sharma, G. Sawhney, S. Kanwar, R. K Gupta, Mod. Phys. Lett. A **25** (2010) 2022.

[12] K. Sandhu, G. Kaur and M. K. Sharma, Nucl. Phys. A **921** (2014) 114.

[13]. N. K. Skobelev, A. A. Kulko, V. Kroha, V. Burjan, Z. Hons, A. V. Daniel et.al., J. Phys. G: Nucl. Part. Phys. **38** (2011) 035106.